



The IQ*-Collaboratory Tjitske Starckenburg

*Isolated and Quiescent galaxies (Northwestern University)

Apples-to-apples comparisons of theoretical and observed galaxy populations: *how much can we learn?*

In collaboration with: Chang Hoon Hahn (Princeton), Claire Dickey (Yale), Ena Choi (KIAS), Kartheik Iyer (Dunlap), Daniel Angles-Alcazar (UConn), Rachel Somerville (Rutgers/CCA), Ari Maller (CUNY), Romeel Dave (ROE), Shy Genel (CCA/Columbia), Chris Hayward (CCA), Marla Geha (Yale), Greg Bryan (Columbia), Jeremy Tinker (NYU), Mika Rafieferantsoa (UWC), Viraj Pandya (UCSC), Gergo Popping (ESO), Nir Mandelker (HUJI), Aaron Yung (Goddard)

Logo credit: Claire Dickey

The physics of galaxy quenching is one of the big open questions in the field of galaxy formation. Observational as well as theoretical approaches have made great strides in this direction. However, to exploit the full scale of the combined observational and theoretical data available requires the application of statistical and data science tools, to perform careful and detailed comparison of the observational data to relevant theoretical models.

The IQ (Isolated & Quiescent) Collaboratory aims to bridge the gap between simulations and observations of star-forming and quiescent galaxies to better characterize internal quenching processes and to compare the variety of implementations of quenching mechanisms in galaxy formation simulations. Our current work includes the development of novel methodology to perform cross-simulation comparisons, to forward model galaxies from multiple large-scale simulations to full mock observational surveys, and to learn about the physics of galaxy formation through detailed and careful, apples-to-apples, comparisons.

This poster illustrates our approach in 4 projects.

The star-forming sequence of simulated central galaxies

A tightly correlated star formation rate (SFR)-stellar mass relation, or star-forming sequence (SFS), is a key feature in galaxy property-space. We present a flexible data-driven approach for identifying this SFS over a wide range of SFRs and stellar masses using Gaussian mixture modeling (GMM) and apply this method to perform a consistent comparison of the $z = 0$ SFSs of central galaxies in the Illustris, EAGLE, and MUFASA hydrodynamic simulations and the Santa Cruz semi-analytic model (SC-SAM), alongside data from the Sloan Digital Sky Survey.

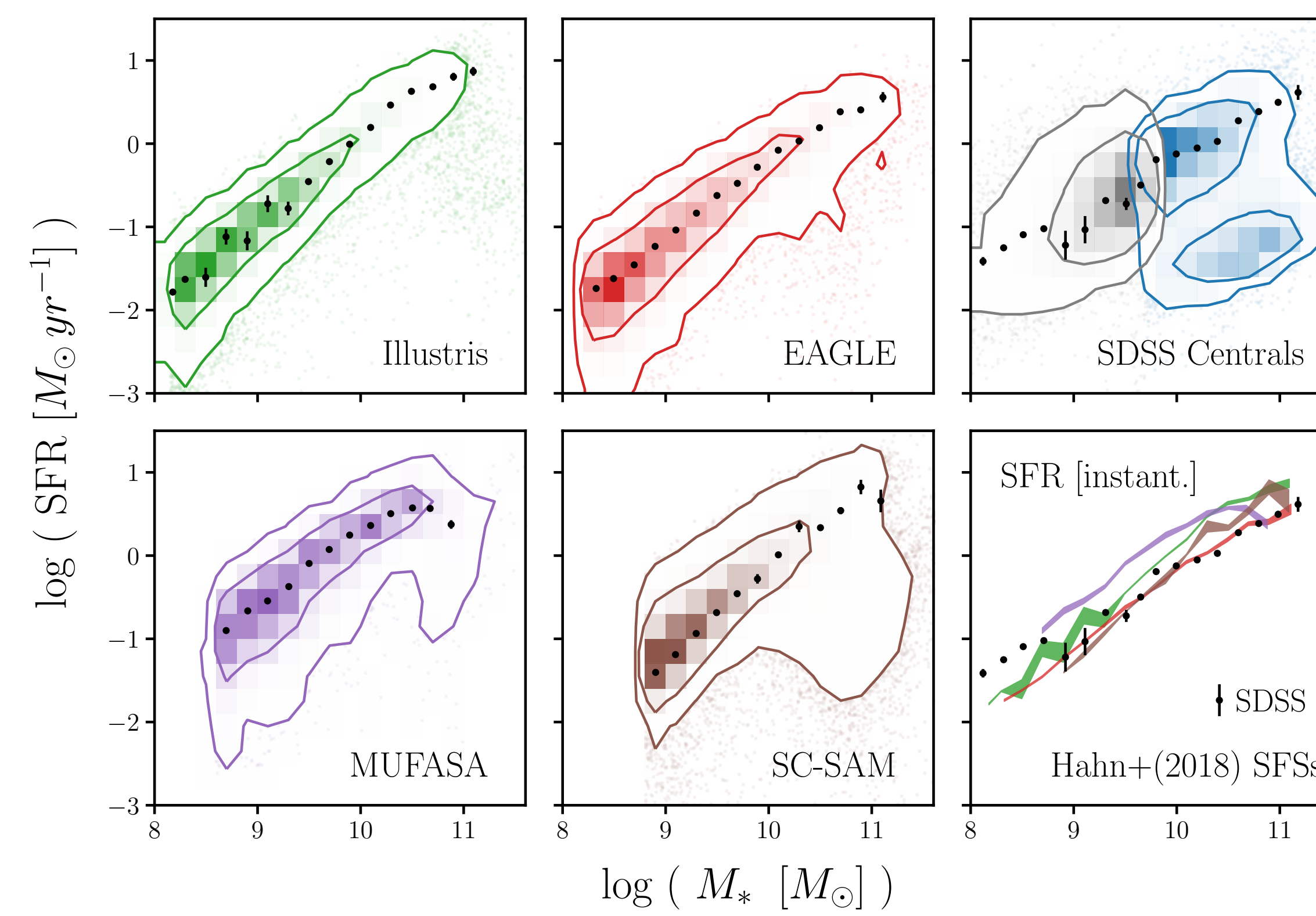


Figure 1: SFSs of the central galaxies in the Illustris, EAGLE, MUFASA, and SC-SAM simulations as identified by our GMM based method. For reference, we include the SFS of the SDSS sample in the top right panel and the bottom right panel (black). When we compare the SFSs of the simulations we find that their amplitudes vary by up to ~ 0.7 dex, a factor of ~ 5 .

We find approximately similar SFS-slope across all simulations, but surprisingly also a factor of 5 (0.7 dex) discrepancy over the whole stellar mass range (see Fig. 1). This seems in some tension with earlier results (Genel+2014, Somerville & Dave 2014, Furlong+2015, Sparre+2015, Schaye+2015, Dave+2016, Bluck+2016), but is purely due to using one and the same definition for the Star Formation Sequence across all simulations.

Our results illustrate that, even among models that well reproduce many observables of the galaxy population, the $z=0$ SFS and other subpopulations still show differences that can provide constraints on galaxy formation models.

Hahn, TS & the IQ-collaboratory 2019

The galaxy star-forming sequence at higher redshifts

We use Gaussian mixture modeling (GMM), a flexible data-driven approach to identify the SFS over a wide range of star formation rates and stellar masses, in 6 different redshift bins from $z=3$ to $z=0.5$, for 5 simulations and the CANDELS observational dataset (Iyer et al. 2018, 2019).

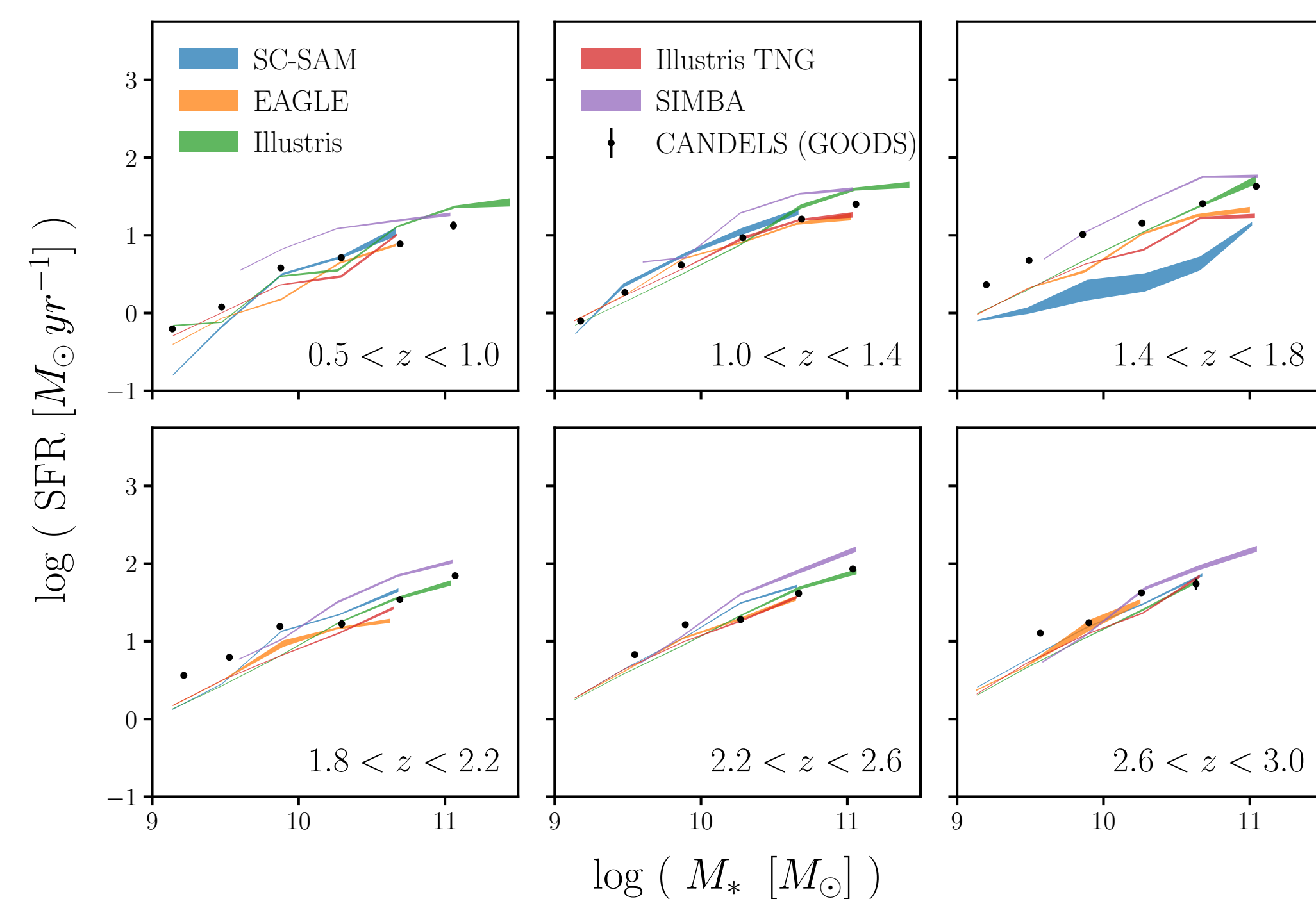


Figure 2: Comparison of the central galaxy SFSs in the SC-SAM, EAGLE, Illustris, IllustrisTNG, and SIMBA simulations, and the CANDELS observations in 6 redshift bins from $z=0.5-3.0$.

We find very good agreement of the location of the galaxy star formation sequence between simulations, in particular at higher redshift, and overall good agreement with CANDELS data (Fig. 3).

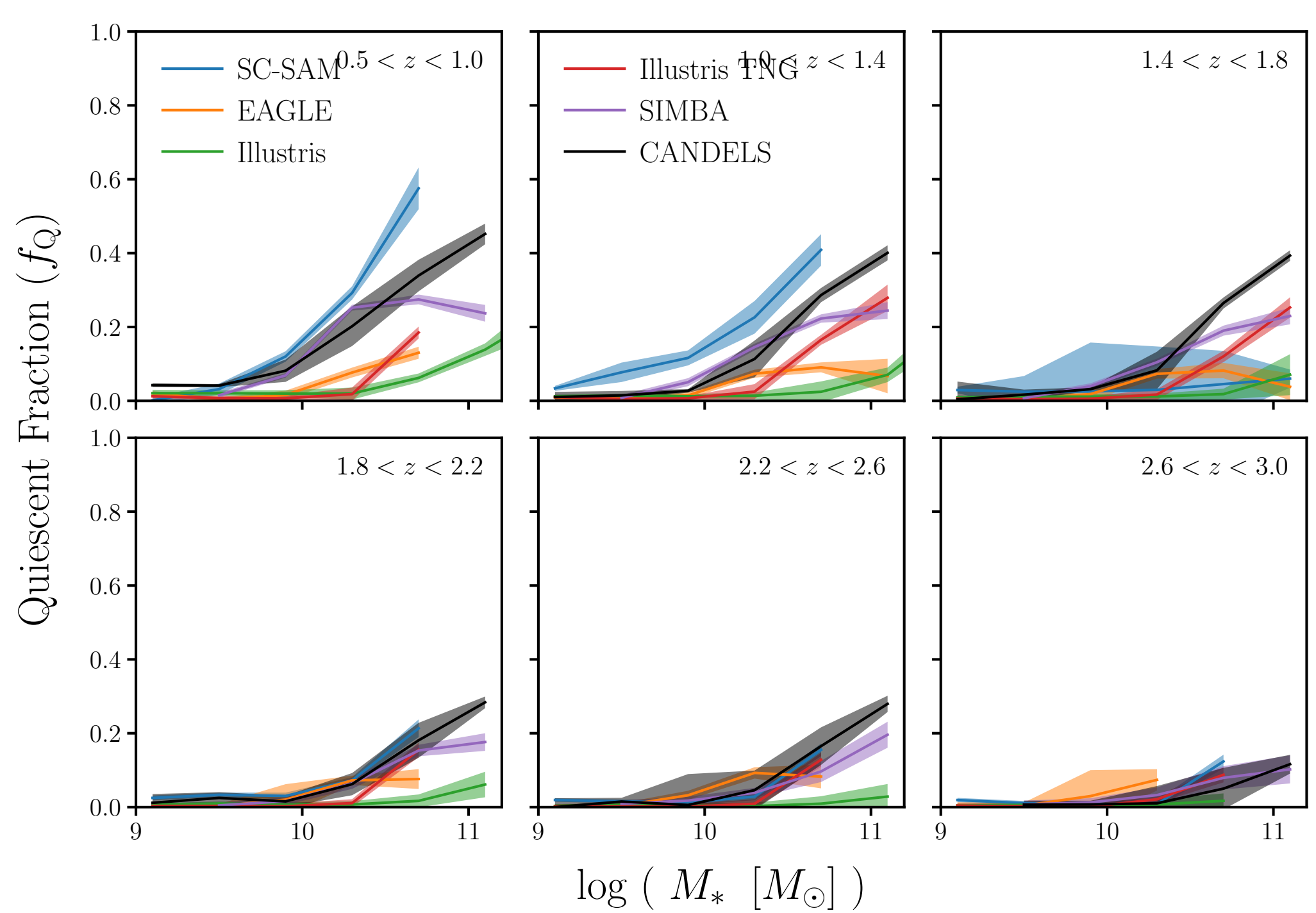


Figure 3: Comparison of the quiescent fraction, i.e. the fractional contribution of the best-fit GMM components below the SFS, of SC-SAM, EAGLE, IllustrisTNG, Illustris, and SIMBA simulations, and CANDELS observations at the 6 redshift bins.

Quiescent fractions based on distance from the SFS are however quite different, and show a variety of trends with stellar mass and especially with redshift evolution across simulations (Fig. 4).

Choi & the IQ-collaboratory in prep.

The low-mass quiescent fraction

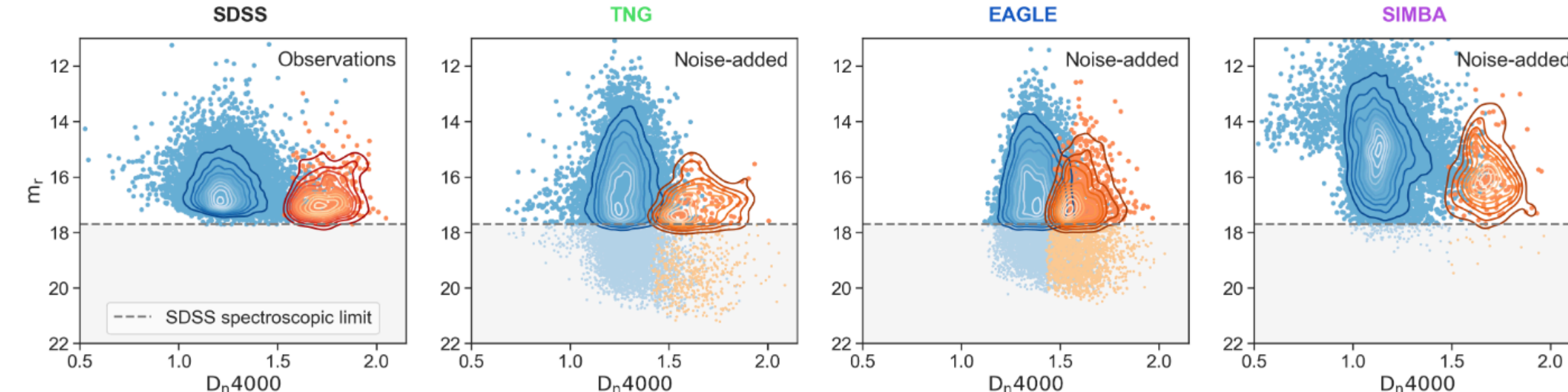


Figure 4: The distribution of apparent r magnitude (m_r) as a function of $Dn4000$. Galaxies are color-coded as star forming (blue) or quiescent (orange) based on the noise-added $H\alpha$ EW and $Dn4000$. Galaxies below the gray dashed line fall below the SDSS spectroscopic limit.

We compare three major large-scale hydrodynamical galaxy simulations (EAGLE, Illustris-TNG, and SIMBA) by forward modeling simulated galaxies into mock SDSS surveys, adding realistic noise and observational limits (see Fig. 4). We re-analyze these mock surveys and compute the fraction of isolated and quiescent low mass galaxies as a function of stellar mass.

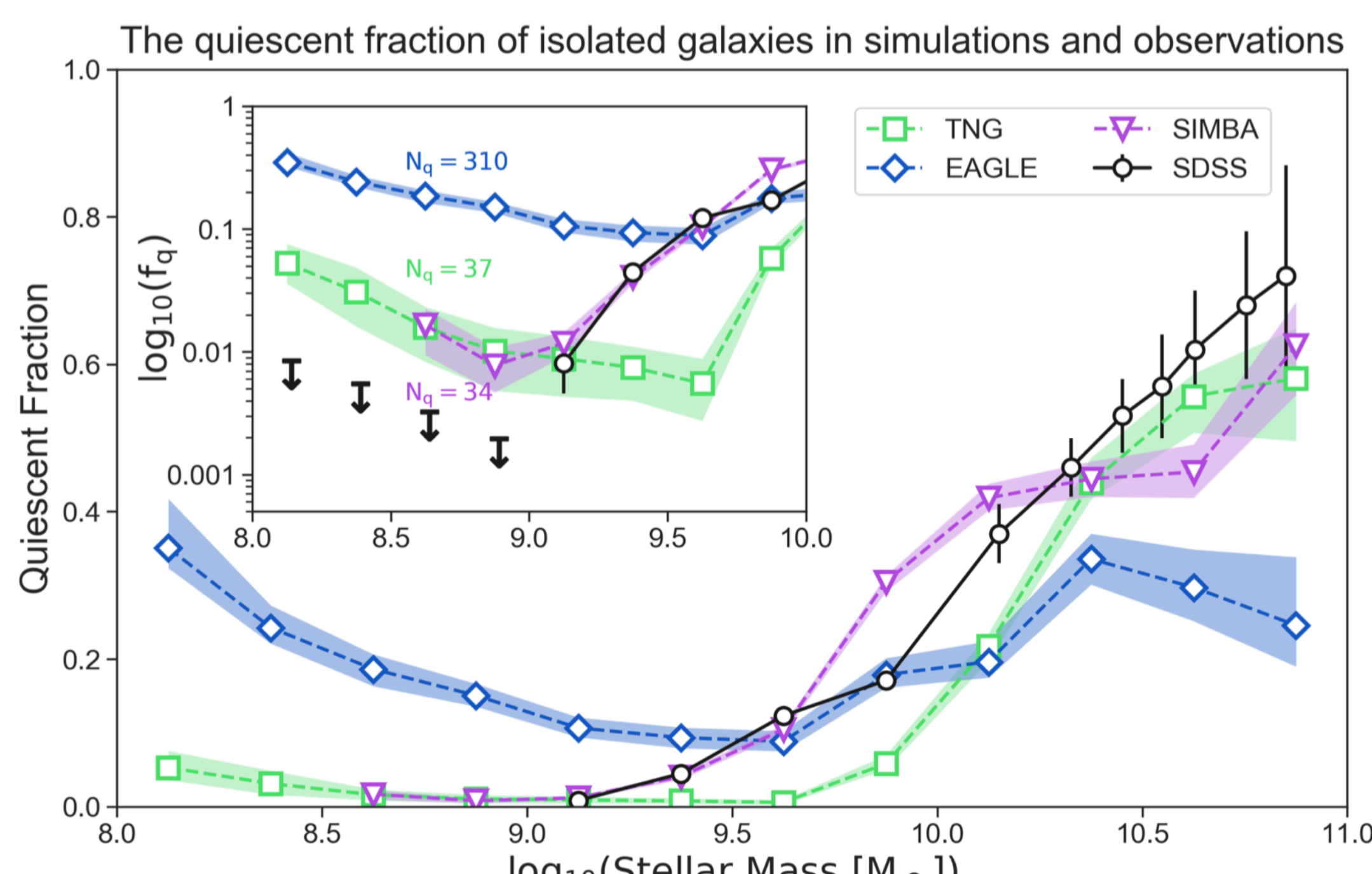


Figure 5: The median quiescent fractions of isolated galaxies as a function of stellar mass for SDSS, Illustris-TNG, EAGLE, and SIMBA. Shaded regions represent the combination of binomial uncertainty on the quiescent fraction and the variance across 25 sightlines for each simulation. Errorbars on the SDSS quiescent fraction are adapted from Geha et al. (2012). Inset: The same data shown in log-scale.

All three simulations show a decrease in the number of quiescent, isolated galaxies in the mass range $M_* = 10^9-10^{10} M_\odot$, in broad agreement with observations. However, even after accounting for observational and selection biases, and possible simulation resolution effects, none of the simulations reproduce the observed absence of quiescent field galaxies below $M_* = 10^9 M_\odot$. This work demonstrates a path towards more robust and accurate comparisons between theoretical simulations and galaxy survey observations, while the quenching threshold serves as a sensitive probe of feedback implementations.

Dickey, TS & the IQ-collaboratory 2020

Taking hydrodynamical simulations with a grain of dust

We present the Empirical Dust Attenuation (EDA), a flexible framework for assigning realistic dust attenuation to simulated galaxies dependent on their physical properties (M_* , sSFR), the Noll+2019 attenuation curve parameterization, and likelihood-free inference based on a comparison of forward modeled synthetic optical and UV observations for a $M_r < -20$ complete galaxy sample with SDSS.

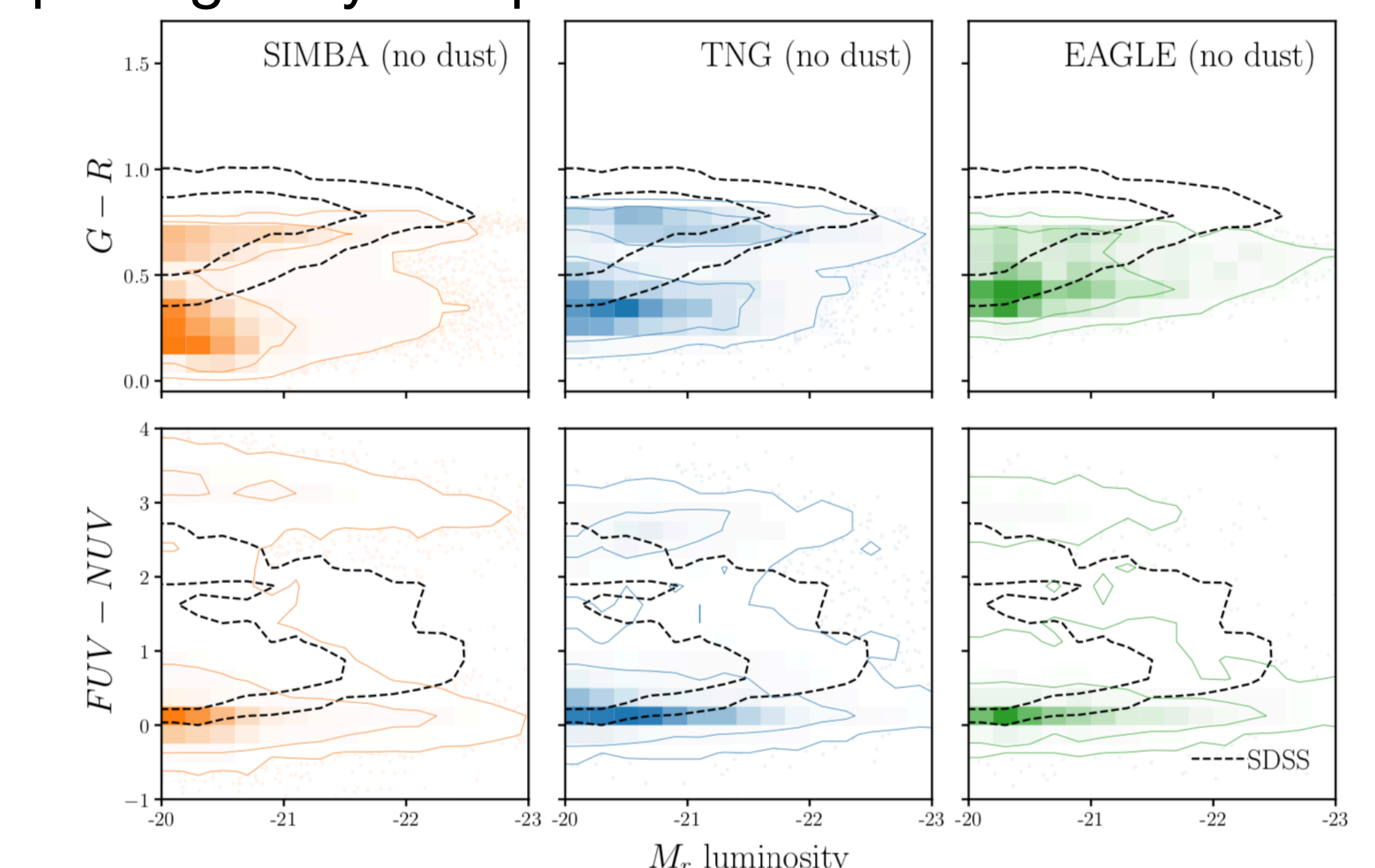


Figure 6: The forward modeled optical and UV color-magnitude relations of SIMBA, TNG, and EAGLE galaxies assuming no dust attenuation. The contours represent the 68 and 95% of the distribution. For comparison, we include the color-magnitude relations of our SDSS sample (black dashed). Without dust attenuation, the hydrodynamical simulations do not reproduce the SDSS color-magnitude relations.

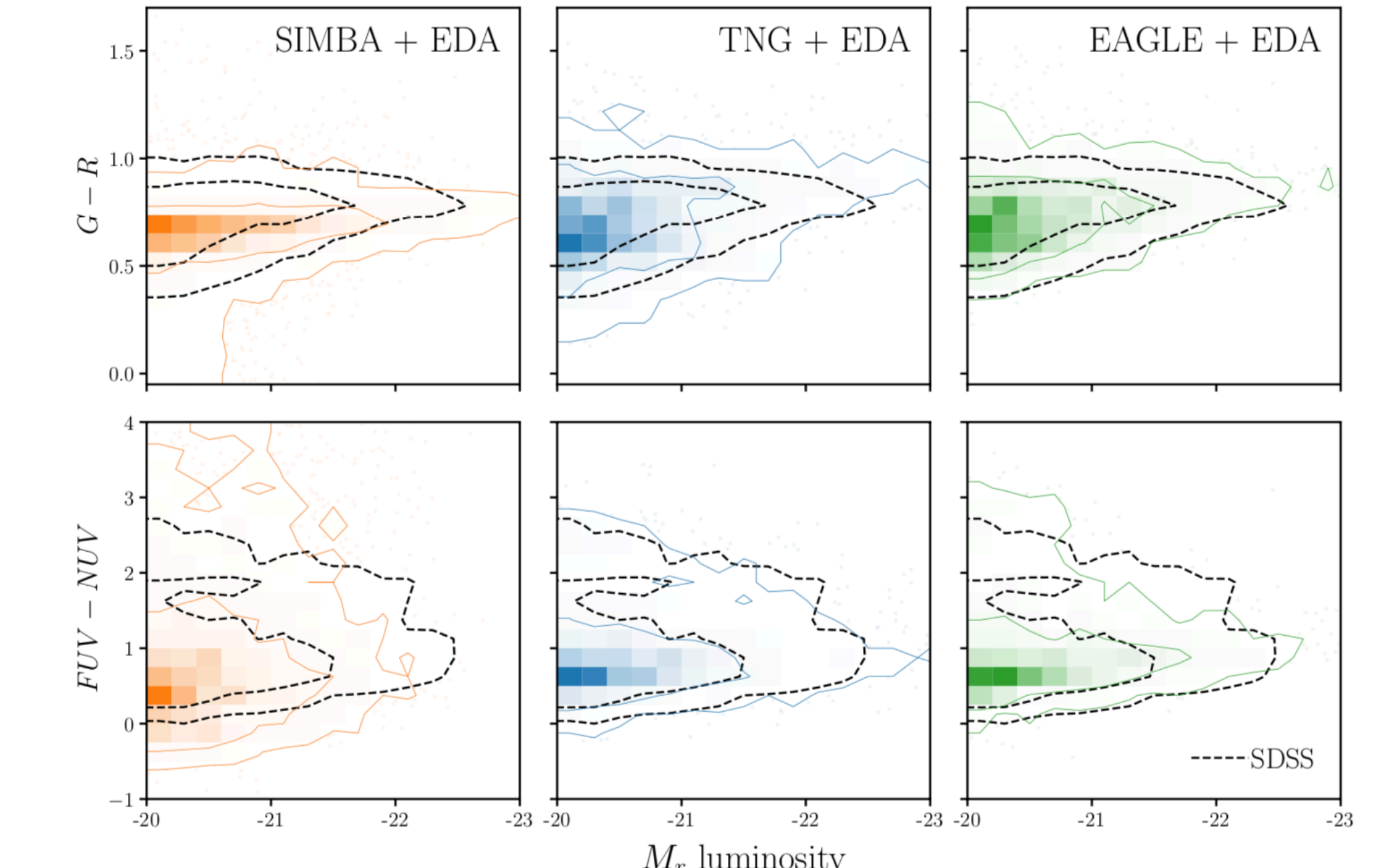


Figure 7: Like figure 6 but including best-fit dust attenuation. Dust dramatically impacts the color-magnitude relations. With our EDA prescription, all three simulations reproduce the color-magnitude relations of SDSS observations.

We find that more massive galaxies in the simulations require higher dust attenuation, while galaxies with higher sSFR have steeper attenuation curves. Additionally, the EDA provides, for the first time, a prediction for attenuation curves of quiescent galaxies. We conclude however, that dust can significantly limit our ability to constrain galaxy formation models.

Hahn, TS & the IQ-collaboratory in prep.